VI. SEPARATION OF R AND THE STRUCTURE FUNCTIONS

VI. A. Interpolation of the Cross Sections

The separation of W_1 and W_2 (or equivalently σ_L and σ_T) at fixed (ν,Q^2) required differential cross sections $\frac{d^2\sigma}{d\Omega dE'}(\nu,Q^2,\theta)$ for at least two values of θ. According to Eq. (I.2), σ_L is the slope and σ_T the $\varepsilon = 0$ intercept of a linear fit to

$$\sum(\nu,Q^2,\theta) = \frac{1}{\Gamma}\frac{d^2\sigma}{d\Omega dE'} = \sigma_T(\nu,Q^2) + \epsilon(\nu,Q^2,\theta)\sigma_L(\nu,Q^2) \quad \text{(VI.1)}$$

The structure functions and R are readily calculated from σ_L and σ_T according to Eqs. (I.3) and (I.4). There were, however only a few kinematic points (ν,Q^2) at which the differential cross sections had been directly measured for two or more values of θ. Consequently, values of Σ and its error were obtained by interpolation of the cross sections measured at each angle to selected kinematic points (ν,Q^2) that fell within the overlaps of two or more of the data triangles measured in experiments A, B, and C. The kinematic region of Q^2 - W^2 space spanned by these overlaps of the measured data triangles is shown in Figure (27). An array of 75 kinematic points (ν,Q^2), chosen to reflect the distribution of measured cross sections, was used in a systematic study of R and the structure functions. As shown in Figure (27), these points lie at the intersections of contours of constant $x(0.1 \leq x \leq 0.8)$ and constant $Q^2(1 \leq Q^2 \leq 16\ \text{GeV}^2)$ with $W > 1.8$ GeV. A subset

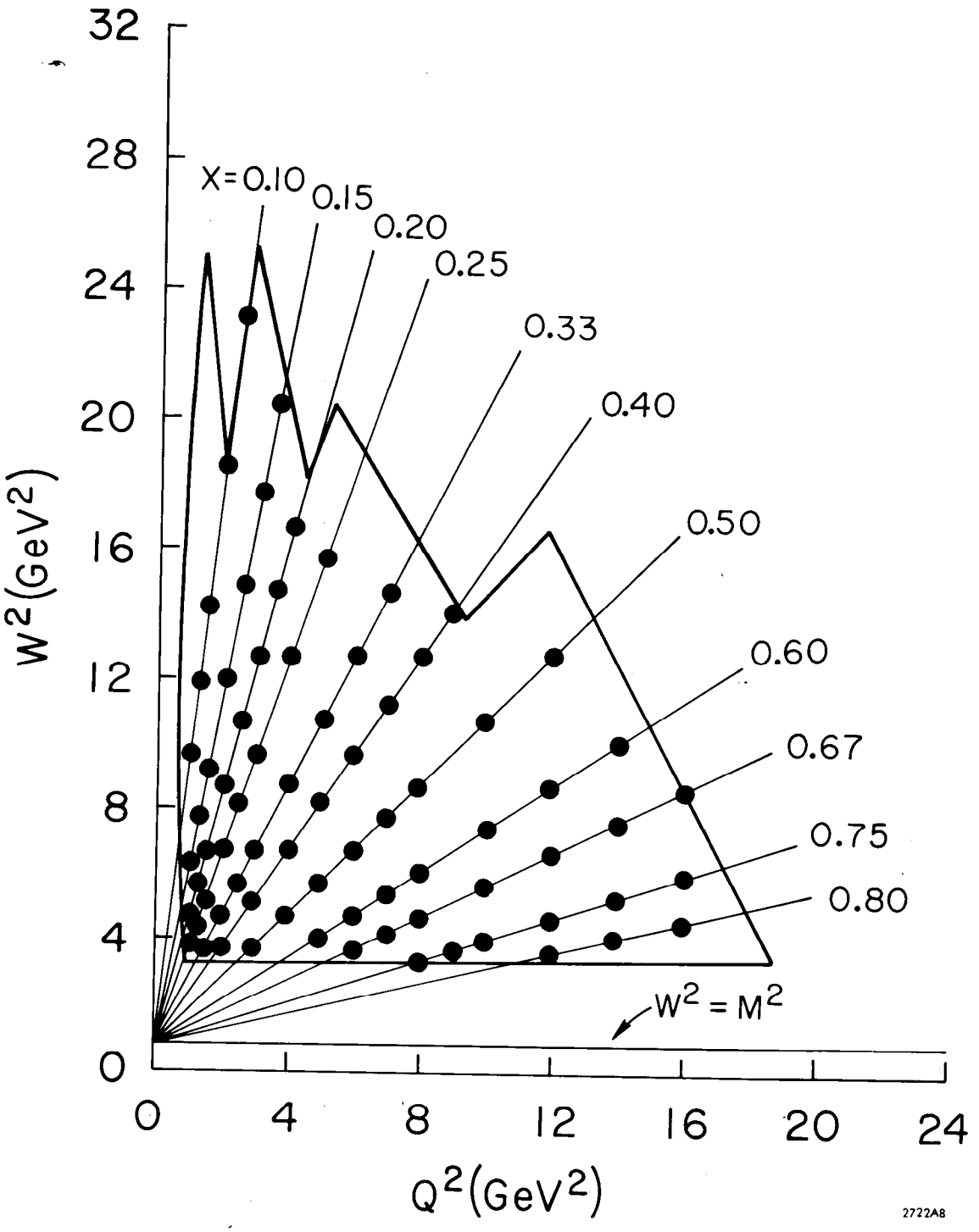

Fig. 27. The kinematic region of $Q^2 - W^2$ space available for the separation of R and the structure functions. Separations were made at the 75 kinematic points (ν , Q^2) shown.

of this $x - Q^2$ array, containing 51 (ν, Q^2) points with $0.2 \leq x \leq 0.8$ and $2 \leq Q^2 \leq 16$ GeV^2, was used in a parallel study wherein only cross sections from experiments A and B were used to extract R and the structure functions. Only the results from the full $x - Q^2$ array are reported here in detail. The results obtained for the restricted $x - Q^2$ array were consistent with those of the full $x - Q^2$ array. Previous separations of R and the structure functions using cross sections from experiments A and C have been reported earlier.[24,27] These previous results are consistent with the present results but are superseded by them.

The e-p and e-d cross sections from Table (V) were used to prepare interpolations at five different values of the scattering angle. As mentioned earlier, all cross sections from experiment B were multiplied by the normalization factor $N_{AB} = 1.010$. In this way, triangles of cross section data were assembled at $\theta = 15^\circ$, 18°, 19°, 26°, and 34°. In order to extend the accessible kinematic region to $x < 0.2$ and to extend the ranges of Q^2 and ε available for $x \geq 0.2$, cross sections measured at 6° and 10° in experiment C were also used in this analysis. These cross sections had been radiatively corrected[27] by the same method as had been used for experiments A and B. Prior to the interpolations, they were multiplied

by $N_{AC} = 1.019$ to normalize them to those of experiment A.

Values of $\Sigma(\nu,Q^2,\theta)$ and its random error were obtained by an interpolation scheme[46], similar to the method used in the radiative corrections, that made no a priori assumptions about the behavior of R. Because this scheme effectively averaged 16 cross section measurements for each (ν,Q^2,θ), the values of $\Sigma(\nu,Q^2,\theta)$ and its errors were correlated for neighboring kinematic points (ν,Q^2). In practice, these correlations were difficult to remove, and the distribution of kinematic points (ν,Q^2) was chosen to minimize them. As many as five values of Σ for five values of ε were available at a given kinematic point (ν,Q^2). In general, the errors of the separated quantities varied inversely as the range $\Delta\varepsilon$ of the variable ε spanned by the cross sections for fixed (ν,Q^2). In the present separations, $\Delta\varepsilon$ ranged from 0.16 to 0.57, while ε itself ranged from 0.24 to 0.98.

VI.B. Separation of R_p and R_d

The quantities σ_L and σ_T were available as the parameters of a linear least square fit to $\Sigma(\nu,Q^2,\theta)$ versus $\varepsilon(\nu,Q^2,\theta)$ at eact kinematic point (ν,Q^2). Sample fits are shown in Figure (28); in general, the confidence level for these fits was quite good. In only a few instances did χ^2 deviate from the number of degrees of freedom n_D of the fit by more than $(2n_D)^{1/2}$. Values of $R = \sigma_L/\sigma_T$ are presented for the proton in Table (XII) along

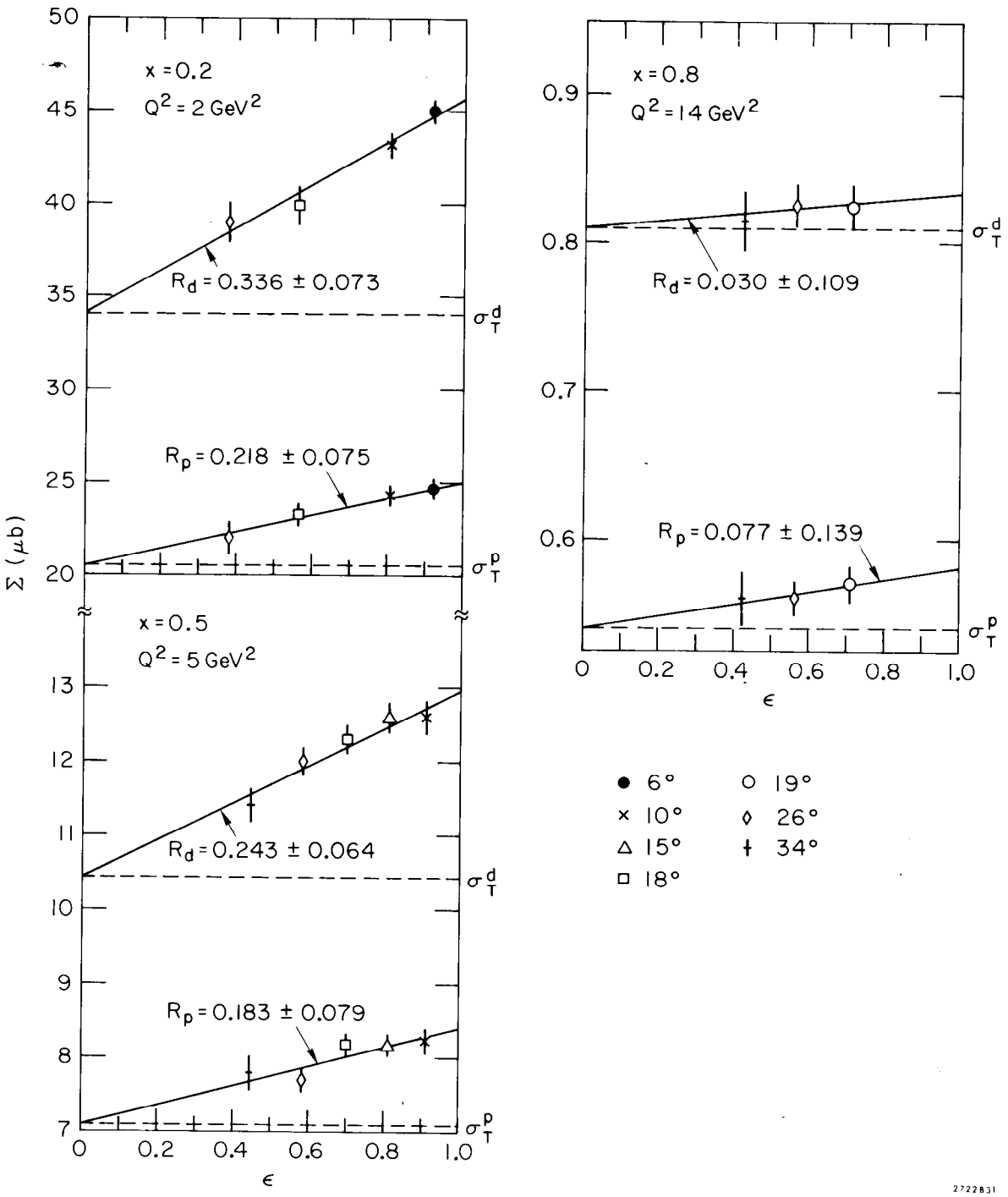

Fig. 28. Sample least square fits to $\Sigma(\nu, Q^2, \theta)$ vs. $\varepsilon(\nu, Q^2, \theta)$ in comparison with data. Σ,ε and the fitting formulas are found in equations I.2 and VI.1. The quantities R and σ_T are available from the fitting parameters and from them, σ_L.

x	Q^2	W	R_p	ΔR_p	ΔR_p^1	ΔR_p^2	ΔR_p^3	ΔR_p^4	ΔR_p^5	R_d	ΔR_d	δ	$\Delta\delta$
0.10	1.00	3.14	0.175±0.132	0.081	0.0	0.036	0.026	0.023	0.063	0.120±0.093	0.082	-0.022±0.171	0.032
0.10	1.25	3.48	0.338±0.155	0.092	0.0	0.036	0.025	0.022	0.078	0.181±0.118	0.074	-0.135±0.200	0.030
0.10	1.50	3.79	0.302±0.127	0.092	0.0	0.034	0.025	0.020	0.079	0.289±0.112	0.087	-0.012±0.184	0.028
0.10	2.00	4.35	0.442±0.199	0.103	0.0	0.028	0.019	0.018	0.096	0.273±0.130	0.090	-0.123±0.232	0.034
0.10	2.50	4.84	0.880±0.844	0.229	0.0	0.115	0.074	0.070	0.171	0.297±0.449	0.182	-0.456±0.881	0.220
0.15	1.00	2.56	0.408±0.159	0.138	0.0	0.094	0.054	0.055	0.064	0.479±0.161	0.167	0.033±0.237	0.090
0.15	1.25	2.82	0.205±0.108	0.102	0.0	0.069	0.038	0.040	0.051	0.377±0.102	0.148	0.201±0.179	0.088
0.15	1.50	3.06	0.095±0.089	0.077	0.0	0.049	0.027	0.028	0.045	0.359±0.118	0.115	0.276±0.203	0.070
0.15	2.00	3.49	0.321±0.096	0.099	0.0	0.061	0.032	0.034	0.063	0.518±0.129	0.131	0.123±0.185	0.065
0.15	2.50	3.88	0.383±0.175	0.130	0.0	0.088	0.042	0.049	0.070	0.471±0.148	0.167	0.078±0.231	0.091
0.15	3.00	4.23	0.332±0.217	0.124	0.0	0.082	0.038	0.045	0.071	0.252±0.142	0.137	-0.060±0.245	0.075
0.15	3.50	4.55	0.174±0.230	0.110	0.0	0.071	0.032	0.033	0.066	0.317±0.173	0.145	0.149±0.303	0.083
0.20	1.00	2.21	0.146±0.107	0.128	0.0	0.097	0.048	0.055	0.039	0.180±0.093	0.108	0.028±0.146	0.098
0.20	1.25	2.42	0.246±0.118	0.136	0.0	0.104	0.048	0.057	0.045	0.267±0.105	0.171	-0.084±0.147	0.086
0.20	1.50	2.62	0.457±0.140	0.151	0.0	0.115	0.049	0.062	0.058	0.483±0.119	0.191	0.009±0.189	0.109
0.20	2.00	2.98	0.218±0.075	0.085	0.0	0.057	0.031	0.033	0.045	0.336±0.073	0.106	0.074±0.113	0.053
0.20	2.50	3.30	0.071±0.072	0.075	0.0	0.054	0.021	0.028	0.037	0.250±0.090	0.109	0.148±0.143	0.062
0.20	3.00	3.59	0.171±0.111	0.098	0.0	0.073	0.028	0.038	0.043	0.277±0.096	0.134	0.102±0.158	0.079
0.20	3.50	3.86	0.261±0.158	0.109	0.0	0.083	0.027	0.042	0.048	0.465±0.151	0.164	0.202±0.244	0.103
0.20	4.00	4.11	0.127±0.122	0.093	0.0	0.071	0.022	0.035	0.043	0.439±0.129	0.154	0.325±0.209	0.102
0.25	1.00	1.97	0.439±0.186	0.255	0.0	0.206	0.086	0.109	0.055	0.426±0.152	0.325	-0.001±0.243	0.194
0.25	1.25	2.15	0.106±0.113	0.135	0.0	0.109	0.044	0.058	0.033	0.184±0.101	0.197	0.063±0.160	0.116
0.25	1.50	2.32	0.307±0.125	0.155	0.0	0.125	0.047	0.065	0.045	0.378±0.109	0.219	0.048±0.170	0.129
0.25	2.00	2.62	0.233±0.083	0.096	0.0	0.072	0.033	0.039	0.038	0.346±0.082	0.129	0.140±0.134	0.078
0.25	2.50	2.89	0.196±0.117	0.103	0.0	0.083	0.025	0.041	0.037	0.316±0.135	0.146	-0.041±0.176	0.070
0.25	3.00	3.14	0.179±0.090	0.089	0.0	0.067	0.030	0.036	0.036	0.242±0.076	0.106	-0.027±0.118	0.056
0.25	4.00	3.59	0.095±0.113	0.074	0.0	0.055	0.023	0.029	0.033	0.174±0.094	0.102	0.097±0.162	0.063
0.25	5.00	3.98	-0.004±0.085	0.066	0.0	0.049	0.018	0.025	0.031	0.096±0.071	0.093	0.130±0.127	0.058
0.33	1.50	1.97	0.475±0.218	0.284	0.0	0.244	0.071	0.117	0.048	0.489±0.170	0.334	-0.006±0.281	0.233
0.33	2.00	2.21	0.121±0.073	0.095	0.0	0.075	0.034	0.040	0.026	0.173±0.062	0.129	0.034±0.098	0.075
0.33	2.50	2.43	0.079±0.102	0.109	0.0	0.095	0.021	0.043	0.028	0.029±0.103	0.128	-0.149±0.136	0.072
0.33	3.00	2.62	0.177±0.058	0.071	0.0	0.051	0.028	0.029	0.027	0.242±0.049	0.090	0.061±0.079	0.049
0.33	4.00	2.98	0.042±0.059	0.060	0.0	0.044	0.023	0.025	0.022	0.217±0.062	0.088	0.188±0.098	0.053
0.33	5.00	3.30	0.041±0.086	0.066	0.0	0.053	0.018	0.026	0.022	0.307±0.092	0.112	0.282±0.156	0.077
0.33	6.00	3.59	0.687±0.346	0.073	0.0	0.0	0.056	0.026	0.038	0.069±0.153	0.045	-0.600±0.263	0.134
0.33	7.00	3.86	0.365±0.339	0.058	0.0	0.0	0.045	0.022	0.031	0.062±0.188	0.046	-0.309±0.316	0.076
0.40	2.00	1.97	0.140±0.085	0.109	0.0	0.088	0.038	0.047	0.023	0.238±0.077	0.156	0.093±0.125	0.096
0.40	3.00	2.32	0.078±0.054	0.064	0.0	0.048	0.027	0.028	0.019	0.137±0.044	0.083	0.055±0.073	0.047
0.40	4.00	2.62	0.193±0.071	0.071	0.0	0.053	0.029	0.031	0.021	0.195±0.054	0.087	-0.000±0.088	0.049
0.40	5.00	2.89	0.106±0.064	0.054	0.004	0.037	0.024	0.024	0.019	0.169±0.055	0.065	0.060±0.090	0.035
0.40	6.00	3.14	0.011±0.058	0.047	0.005	0.034	0.018	0.021	0.017	0.143±0.049	0.066	0.140±0.085	0.040
0.40	7.00	3.37	0.040±0.091	0.048	0.032	0.0	0.024	0.020	0.016	0.166±0.075	0.047	0.131±0.127	0.045
0.40	8.00	3.59	0.166±0.104	0.052	0.033	0.0	0.028	0.022	0.010	0.151±0.074	0.046	0.015±0.127	0.041
0.40	9.00	3.79	0.178±0.208	0.046	0.0	0.0	0.036	0.020	0.019	0.110±0.147	0.044	-0.065±0.248	0.011
0.50	3.00	1.97	0.074±0.060	0.073	0.0	0.057	0.029	0.032	0.014	0.125±0.050	0.094	0.042±0.083	0.057
0.50	4.00	2.21	0.190±0.074	0.067	0.0	0.048	0.032	0.031	0.015	0.181±0.056	0.083	0.002±0.096	0.047
0.50	5.00	2.42	0.183±0.073	0.056	0.006	0.037	0.027	0.028	0.015	0.243±0.064	0.068	0.061±0.106	0.041
0.50	6.00	2.62	0.085±0.062	0.047	0.001	0.032	0.022	0.024	0.012	0.209±0.055	0.066	0.125±0.091	0.040
0.50	7.00	2.81	0.086±0.067	0.048	0.018	0.031	0.019	0.023	0.013	0.176±0.055	0.064	0.094±0.092	0.039
0.50	8.00	2.98	0.040±0.087	0.032	0.007	0.0	0.019	0.021	0.012	0.243±0.081	0.040	0.201±0.134	0.048
0.50	10.00	3.30	0.217±0.130	0.052	0.032	0.0	0.032	0.022	0.013	0.138±0.086	0.044	-0.013±0.158	0.023
0.50	12.00	3.59	0.184±0.150	0.040	0.0	0.0	0.031	0.023	0.013	0.170±0.119	0.040	0.004±0.194	0.033
0.60	5.00	2.05	0.231±0.100	0.058	0.026	0.026	0.031	0.031	0.011	0.058±0.061	0.046	-0.176±0.104	0.042
0.60	6.00	2.21	0.240±0.083	0.057	0.002	0.030	0.026	0.030	0.012	0.108±0.055	0.052	-0.134±0.034	0.036
0.60	7.00	2.36	0.091±0.061	0.050	0.005	0.037	0.019	0.025	0.010	0.110±0.049	0.061	0.020±0.082	0.036
0.60	8.00	2.49	0.149±0.088	0.033	0.006	0.0	0.020	0.024	0.009	0.163±0.072	0.035	0.032±0.114	0.044
0.60	10.00	2.75	0.109±0.081	0.028	0.003	0.0	0.010	0.025	0.008	0.119±0.070	0.029	0.017±0.107	0.046
0.60	12.00	2.98	0.001±0.120	0.030	0.0	0.0	0.022	0.019	0.007	0.120±0.109	0.034	0.127±0.171	0.052
0.60	14.00	3.20	0.034±0.110	0.030	0.0	0.0	0.020	0.021	0.007	0.053±0.099	0.029	0.024±0.155	0.038
0.67	6.00	1.97	0.238±0.130	0.047	0.001	0.019	0.023	0.034	0.009	0.063±0.082	0.037	-0.148±0.146	0.054
0.67	7.00	2.09	0.182±0.081	0.052	0.001	0.037	0.020	0.030	0.008	0.084±0.058	0.047	-0.076±0.101	0.035
0.67	8.00	2.21	0.244±0.093	0.048	0.031	0.0	0.020	0.029	0.007	0.035±0.058	0.032	-0.209±0.097	0.045
0.67	10.00	2.42	0.107±0.088	0.030	0.006	0.0	0.011	0.026	0.008	0.082±0.071	0.028	-0.030±0.110	0.040
0.67	12.00	2.62	-0.016±0.091	0.035	0.023	0.0	0.016	0.020	0.005	0.073±0.080	0.035	0.087±0.126	0.014
0.67	14.00	2.81	0.058±0.111	0.029	0.0	0.0	0.017	0.022	0.005	0.176±0.103	0.032	0.114±0.158	0.051
0.67	16.00	2.98	0.351±0.284	0.036	0.0	0.0	0.002	0.036	0.007	-0.005±0.168	0.026	-0.345±0.263	0.085
0.75	8.00	1.88	0.215±0.187	0.043	0.002	0.0	0.008	0.042	0.006	0.378±0.198	0.053	0.211±0.338	0.135
0.75	9.00	1.97	0.165±0.108	0.033	0.002	0.0	0.003	0.033	0.005	0.122±0.086	0.031	-0.021±0.147	0.057
0.75	10.00	2.05	0.189±0.108	0.033	0.007	0.0	0.015	0.028	0.005	0.071±0.077	0.030	-0.112±0.130	0.044
0.75	12.00	2.21	0.108±0.103	0.035	0.019	0.0	0.015	0.024	0.004	0.098±0.080	0.033	0.007±0.133	0.016
0.75	14.00	2.36	0.100±0.115	0.028	0.0	0.0	0.016	0.023	0.004	0.153±0.101	0.030	0.052±0.155	0.054
0.75	16.00	2.49	0.132±0.114	0.028	0.0	0.0	0.010	0.026	0.004	0.267±0.107	0.032	0.128±0.166	0.057
0.80	12.00	1.97	0.022±0.138	0.026	0.008	0.0	0.009	0.023	0.003	0.152±0.127	0.030	0.140±0.210	0.035
0.80	14.00	2.09	0.077±0.139	0.027	0.0	0.0	0.003	0.025	0.003	0.030±0.109	0.025	-0.004±0.166	0.042
0.80	16.00	2.21	0.142±0.124	0.028	0.0	0.0	0.005	0.028	0.003	0.165±0.104	0.028	-0.014±0.160	0.043

2722C26

Table XII. Separated values of R_p, R_d, and δ with their random errors and systematic uncertainties. The quantities ΔR_p and ΔR_p^j are discussed in the text.

with statistical errors and estimates of the systematic uncertainty ΔR_p. The five contributions to the total systematic uncertainty ΔR_p are listed separately in Table (XII). The uncertainty ΔR_p^1 arising from the uncertainty of 0.010 in N_{AB}^p was estimated by repeating the separations using instead a normalization factor $N_{AB}^p = 1.020$. A similar procedure was used to estimate the uncertainty ΔR_p^2 arising from the uncertainty of 0.017 in N_{AC}^p. The uncertainty ΔR_p^3 arising from a possible E' dependence of the spectrometer acceptance was estimated[25] by using a redefined acceptance that varied by at most 1% from its nominal value (see Appendix 1). The uncertainty ΔR_p^4 due to relative uncertainties in detector efficiencies was estimated by using redefined efficiencies that varied from their nominal values by at most 1% (at E' = 2 GeV). The radiative correction uncertainty ΔR_p^5 was estimated by varying all proton cross sections by an amount $\Delta\sigma$ determined according to equation (IV.7). These five contributions were added in quadrature to obtain the total uncertainty ΔR_p reported in Table (XII). The present values of R_p are consistent with those reported earlier[25, 27]; much more accurate data are presented for $\omega \lesssim 2$ than were available before.

Values of R_d are also listed in Table (XII); they were extracted from the interpolated deuteron cross sections using the same procedure as used for the proton. The five contributions to the systematic uncertainty in R_d were calculated

in the same manner as used for R_p, except that uncertainties of 0.007 and 0.024 in the deuteron normalization factors N^d_{AB} and N^d_{AC} were used. They were added in quadrature to obtain the total uncertainty ΔR_d listed.

The weighted averages of R_p and R_d over the full $x - Q^2$ array provide a rough comparison of these quantities. We find $\bar{R}_p = 0.138 \pm 0.011$, with a total systematic uncertainty $\Delta\bar{R}_p = 0.056$, and $\bar{R}_d = 0.175 \pm 0.009$, with a total systematic uncertainty $\Delta\bar{R}_d = 0.060$. Within the normalization uncertainty of experiment C alone, $\bar{R}_d$ is consistent with being equal to $\bar{R}_p$. When the weighted averages are taken over the restricted $x - Q^2$ array only, using data from experiments A and B, we find $\bar{R}_p = 0.136 \pm 0.017$ and $\bar{R}_d = 0.137 \pm 0.013$.

A more detailed and accurate comparison of R_p, R_d, and R_n was achieved by extracting the quantity $\delta = R_d - R_p$ from the ratio of differential cross sections σ_d/σ_p in a method that exploited the expected small systematic uncertainty in this ratio. From Eq. (I.2) we get[26]

$$\frac{\sigma_d}{\sigma_p} = \frac{\sigma_{Td} + \epsilon\sigma_{Ld}}{\sigma_{Tp} + \epsilon\sigma_{Lp}} = T\frac{(1+\epsilon R_d)}{(1+\epsilon R_p)} = T(1+\epsilon'\delta) \qquad \text{(VI.2)}$$

where $T = \sigma_{Td}/\sigma_{Tp}$ and $\epsilon' = \epsilon/(1 + \epsilon R_p)$. The physical meaning of Equation (VI.2) is clear: a difference between R_d and R_p results in a slope in σ_d/σ_p plotted versus ϵ'(or, essentially versus ϵ). The connection between R_n and δ is achieved through an expression[20] that exploits the observation that the smearing correction is empirically the same for W_1 and W_2 (see

Appendix III)

$$R_d = R_p\left(\frac{1}{1+Z}\right) + R_n\left(\frac{Z}{1+Z}\right) \qquad \text{(VI.3 a)}$$

$$R_n = R_d + \delta/Z \qquad \text{(VI.3 b)}$$

where $Z = W_{1s}^n/W_{1s}^p$ is the ratio of smeared W_1^n to smeared W_1^p. In practice, Eq. (VI.3 b) is not very useful if $\delta \neq 0$, for Z is also an unknown. But if $\delta=0$, which we find to be consistent with our overall results, then $R_n = R_d$ and $R_n = R_p$. In this manner we can compare R_p, R_d, and R_n, independent of the assumptions about R_n needed to calculate σ_n from σ_d in the impulse approximation.

At each of the 75 kinematic points (ν,Q^2), the quantity δ was extracted as one of the two parameters of a least square fit of the form of Eq. (VI.2) to interpolated values of σ_d/σ_p versus ε'. The interpolations program was almost identical to the one used to interpolate Σ. At each (ν,Q^2) point, the value of R_p in $\varepsilon' = \varepsilon/(1 + \varepsilon R_p)$ was taken to be that listed in Table (XII). Values of δ and its random error from these fits are reproduced in Table (XII) along with estimates of the total systematic uncertainty $\Delta\delta$. One contribution to this uncertainty arose from the ambiguity in the appropriate choice of R_p used to calculate ε' and ranged from 0.0 to 0.02 in δ. Another uncertainty arose from the uncertainty of 1.3% in the

ratic of deuteron to proton normalization factors N_{AB}^{d}/N_{AB}^{p} and ranged from 0.01 to 0.12 in δ. A third uncertainty in δ arose from taking the normalization factor N_{AC}^{d} to be equal to N_{AC}^{p}, which had been calculated by a comparison of elastic e-p cross sections; this uncertainty ranged from 0.02 to 0.23 in δ. The quadratic sum of these three uncertainties is presented in Table (XII) as $\Delta\delta$ and is, in general, much smaller than the random error in δ.

The result $\delta = 0$ is consistent with all the data listed in Table (XII). Values of δ are typically less than one standard deviation, and in only two instances more than two standard deviations, different from zero. Weighted averages of δ for each of the 11 values of x are presented in Figure (29) along with their random errors. Systematic uncertainties in these averages range from 0.03 to 0.08 and are largest for the range $0.15 \leq x \leq 0.33$. No statistically significant deviation from zero can be seen anywhere in these data. When the normalization factor N_{AC}^{d} was taken to be unity instead of 1.019, the average values of δ in the range $0.10 \leq x \leq 0.50$ were all within one standard deviation of zero. The average of δ over the full $x - Q^2$ array, $\bar{\delta} = 0.031 \pm 0.015$, has a total systematic uncertainty of $\Delta\delta = 0.036$ and is consistent with zero. If δ is calculated using only cross sections from experiments A and B, its average over the restricted $x - Q^2$ array is $\delta = -0.001 \pm 0.022$. The only suggestion of some non-zero be-

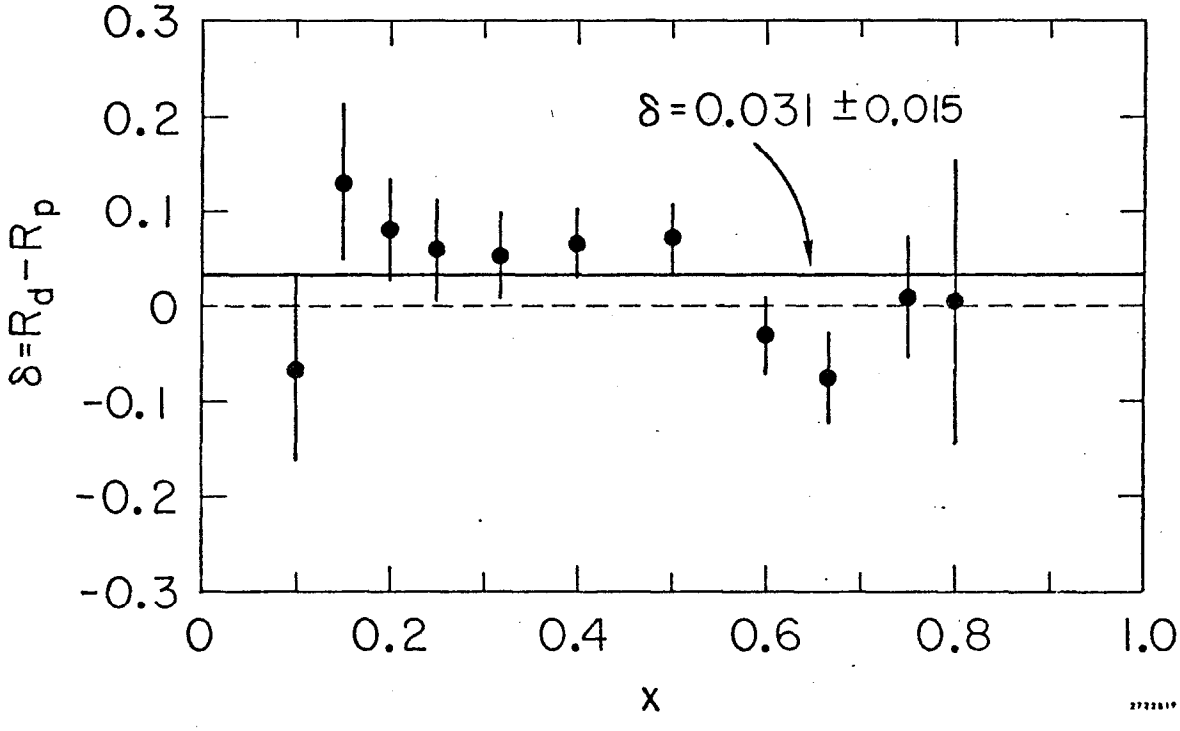

Fig. 29. Average values of the quantity $\delta = R_d - R_p$ for each of the 11 values of x studied. Errors shown are purely random. The systematic error in $\bar{\delta}$ is 0.036.

havior of δ occurs for $W \lesssim 2.5$ GeV and $x \geq 0.60$, where R_d is consistently smaller than R_p. Present estimates of the off-mass-shell corrections to the deuteron smearing ratios (see Reference (63) and Appendix (III)) are much smaller than the errors in R_d and cannot explain this effect. Except for this possible difference at low W, which could be influenced by tails from the nucleon resonances, we conclude that $R_d = R_p$, and hence that $R_n = R_p$, over the full range of the $x - Q^2$ array.

VI.C. Kinematic Variation of R_p and R_d

The behavior of R in the Bjorken limit is an important test of constituent models[6, 21] of nucleon structure. In conventional field theories with only spin-1/2 charged constitutents, R should vanish as $1/Q^2$ in the Bjorken limit.[21,22] More recently, field theories with asymptotic freedom[18] predict that R should vanish as $1/\log Q^2$. In both cases, the presence of charged spin-0 constituents would be reflected in a non-vanishing contribution to R, i.e., R itself should scale.[23] The kinematic variation of R was, however, difficult to ascertain because of large random errors and systematic uncertainties in the present data. Consequently, two approaches to the study of the kinematic variation of R_p and R_d were used. In the first approach, universal fits were made to the entire body of data for R_p or R_d. In the second approach, individual

fits to R_p or R_d were attempted at each of the 11 values of x at which these quantities were available. The interpretation of these fits is discussed in this section.

The results of four least square fits to all the data for R_p and R_d are presented in Table (XIII). Included in the table are the best fit parameters, their random errors and systematic uncertainties, and the χ^2 sum for each fit. Systematic uncertainties in the fit parameters arising from the five uncertainties in R_p or R_d were added in quadrature to produce the numbers listed under Δ in Table (XIII). When only the R_p or R_d data for $W \geq 2.0$ GeV were used in these fits, the best fit parameters shifted by less than one standard deviation.

The χ^2 for the universal fits to R_p was consistently smaller than the χ^2 for the corresponding fits to the R_d data. This fact probably reflects the fact that the random errors for R_d are smaller, relative to the systematic uncertainties, than those for R_p. In addition to the fits listed in Table (XIII), fits of the forms $R = cQ^2$, $R = cQ^2(1-x)^2$, $R = Q^2/\nu^2$ were attempted. These functions provided very poor fits to the data, and are consequently not listed. Except at low $x \lesssim 0.2$, the data for R_p and R_d are inconsistent with a linear rise in Q^2, as required by simple vector dominance models[13] of inelastic e-N scattering. A constant value still fits the R_p data quite well. The best-fit value $R_p = 0.14 \pm 0.07$ is consistent with

Table XIII. Universal fits to R_p and R_d. The best fit parameters for each fit function are listed along with the total χ^2 of the fits to 75 data points. The quantity Δ represents the systematic uncertainty in each parameter.

Fit function	Proton Best-fit parameter	Δ	χ^2	Deuteron Best-fit parameter	Δ	χ^2
$R=c$	c =0.138 0.011	0.056	71	c =0.175 0.009	0.060	107
$R=\frac{Q^2}{\nu^2}(c+\frac{d}{x^2})$	c =0.392 0.100 d =0.073 0.012	0.152 0.041	63	c =0.334 0.080 d =0.108 0.010	0.135 0.056	116
$R=\frac{cQ^2}{(Q^2+d^2)^2}$	c_2=0.861 0.202[a] d^2=0.988 0.388[a]	0.363[a] 0.229[a]	62	c_2=1.281 0.167[a] d^2=1.158 0.241[a]	0.399[a] 0.289[a]	73
$R=\frac{c}{1+d\cdot\ln(\frac{Q^2}{M^2})}$	c =0.294 0.063 d =0.808 0.358	0.165 0.237	58	c =0.355 0.045 d =0.665 0.184	0.206 0.261	77

[a] in units of GeV^2

the values $R_p = 0.18 \pm 0.10$ and $R_p = 0.16 \pm 0.10$ reported in earlier determinations[7, 24] of this quantity over different kinematic ranges. On the basis of χ^2, a constant fit to the R_d data fares rather poorly, but this may reflect only the influence of systematic uncertainties, particularly in the deuteron normalization factor N_{AC}^d. The strict Callan-Gross relation[21] $R = Q^2/\nu^2$ fits both proton and deuteron data very poorly, and the form $R = cQ^2/\nu^2$ is only marginally better. However, a more general spin-1/2 prediction[22, 23] $R = g(x)Q^2/\nu^2$ provides an excellent representation of the R_p data and a fair representation of the R_d data. Such a deviation from simple Q^2/ν^2 behavior at large ω has been predicted from Regge arguments[22] in the framework of light-cone algebras[21], and deduced[67] from ρ-electroproduction data.[68] The fitting function[69] $R = cQ^2/(Q^2 + d^2)^2$ insures that $R \to 0$ as $Q^2 \to 0$, as required by gauge invariance, and vanishes as $1/Q^2$ in the Bjorken limit. It provides excellent fits to both the proton and deuteron data. A similar[69] fit, $R = cQ^2/(Q^2 + d^2)$, that vanishes as $Q^2 \to 0$ and approaches a constant in the Bjorken limit, fits the R_p and R_d data with equally good χ^2. However, the best fit values of d^2 are negative producing singularities in R_p and R_d at $Q^2 = -d^2$, and the fit is not included in Table (XIII). The final fit is derived from $R = \dfrac{\alpha}{\ln(Q^2/\beta^2)}$, with $d = \left(\ln\dfrac{M^2}{\beta^2}\right)^{-1}$ and $c = \alpha^2 d$. While

this fit is necessarily singular at $Q^2 = \beta^2$, or at $Q^2 = 0.255$ GeV^2 for the proton and $Q^2 = 0.196$ GeV^2 for the deuteron, the model is intended to apply in the limit of high Q^2. This function fits the data equally as well as $R = cQ^2/(Q^2 + d^2)^2$, and the present data cannot distinguish between an asymptotic $1/Q^2$ and $1/\log Q^2$ behavior of R in the Bjorken limit. Although these two functional forms fit the data better than the constant fit, we cannot rule out a non-vanishing contribution to R, at least not on the basis of the universal fits to all the present data. For a sample of data restricted to $x \geq 0.25$, the constant, the asymptotic $1/Q^2$ and the $1/\log Q^2$ functions all fit R_p equally well, while the constant fit is still a poor representation of the data for R_d.

The $x - Q^2$ array permitted a study of the Q^2-dependence of R_p and R_d for fixed values of x in the range $0.1 \leq x \leq 0.8$. This approach allowed unbiased tests of functional forms that could not be fitted satisfactorily to the overall x-dependence of R, and consequently allowed more stringent tests of the behavior of R_p and R_d in the Bjorken limit for various regions of x. The data for R_p and R_d are plotted versus Q^2 in Figure (30) for the 11 fixed values of x available. The three curves plotted at each x in these figures represent best fits of the functional forms $R = c(x)$, $R = \alpha^2(x)/\log(Q^2/\beta^2)$, and $R = c(x)Q^2/(Q^2 + d^2)^2$, corresponding to three of the universal fits reported in Table (XIII).

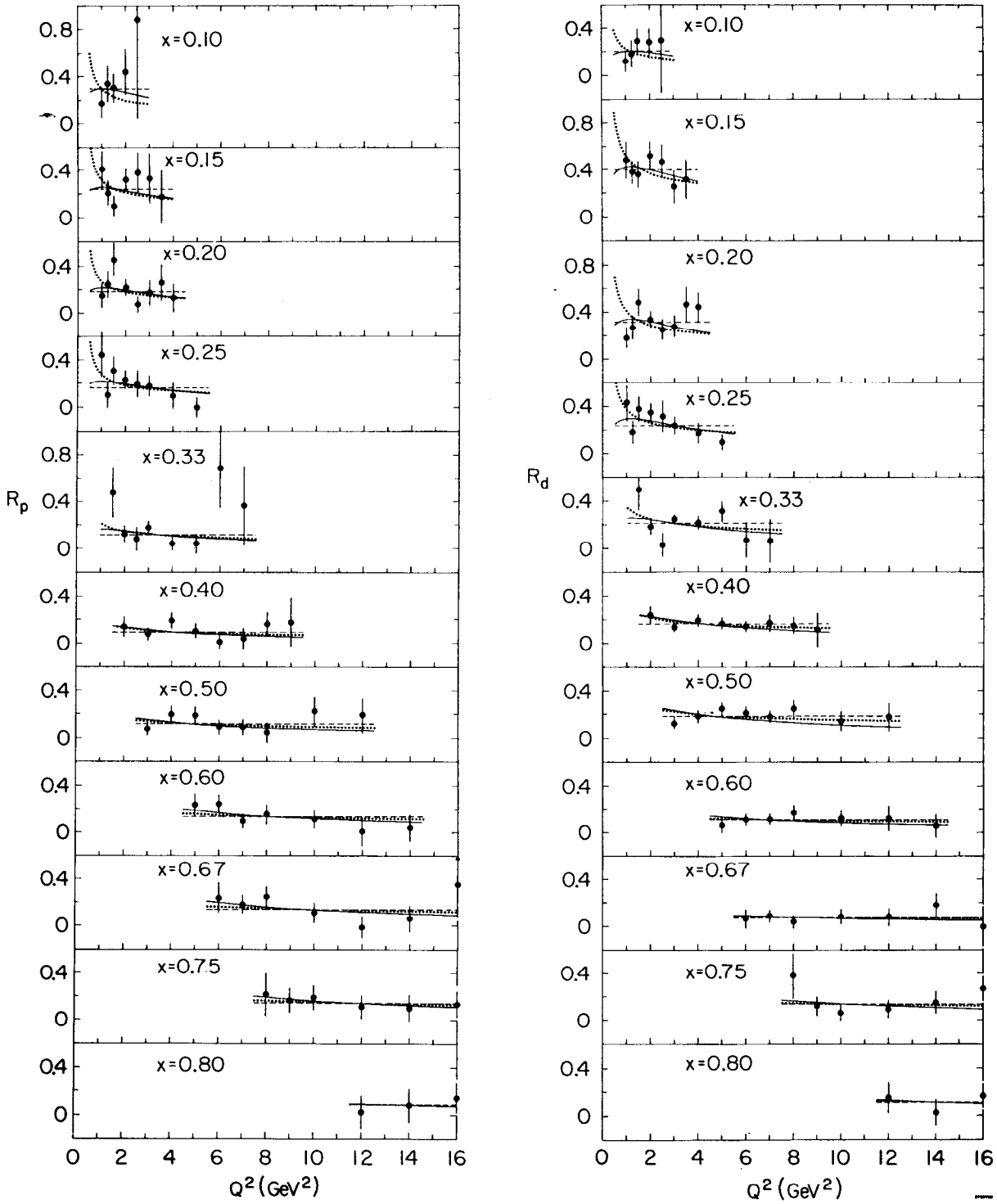

Fig. 30. The values R_p and R_d plotted against x for the 11 values of x studied. Errors shown are purely random. The dashed lines represent constant fits to R_p and R_d at each value of x. The solid lines and dotted lines represent fixed-x fits of the form $R = c(x)Q^2/(Q^2+d^2)^2$ and $R = \alpha^2(x)/\ln(Q^2/\beta^2)$ at each value of x.

The two parameters β^2 and d^2 were set equal to the corresponding parameters of the universal fits in Table (XIII). The best fit parameters of these fits are plotted versus x in Figure (31), and the total χ^2 for the 11 fixed-x fits (64 degrees of freedom) of each function are also given. The solid lines in this figure represent the values of the best-fit parameters of the corresponding universal fits from Table (XIII). Fixed-x fits of other functional forms were also attempted. In particular, a form $R = c(x)/Q^2$ fits the R_p data well for $x \geq 0.25$ but has less than 20% confidence for $x \leq 0.2$. The form $R = c(x)Q^2$ is consistent with the data for $x \leq 0.2$, but is a very poor fit at higher x. Over the full range of x, it is difficult to distinguish among the constant, the asymptotic $1/Q^2$, and the $1/\log Q^2$ fits to R. The relatively large values of χ^2 obtained in the constant universal fits can be seen to be the result of a slow variation of R with x. For both the proton and deuteron, R varies from about 0.3 at low values of x to about 0.1 at the high values of x reported. On the other hand, the success of the universal $1/\log Q^2$ fit can be attributed to the fact that it accomodates, perhaps fortuitously, this x-variation of R_p and R_d quite well. The modified $1/Q^2$ universal fit also represents the low-x, low-Q^2 behavior of R_p and R_d fairly well, and provides an equally good fit as $1/\log Q^2$ to all the data. In summary, the present data for R_p and R_d are consistent with

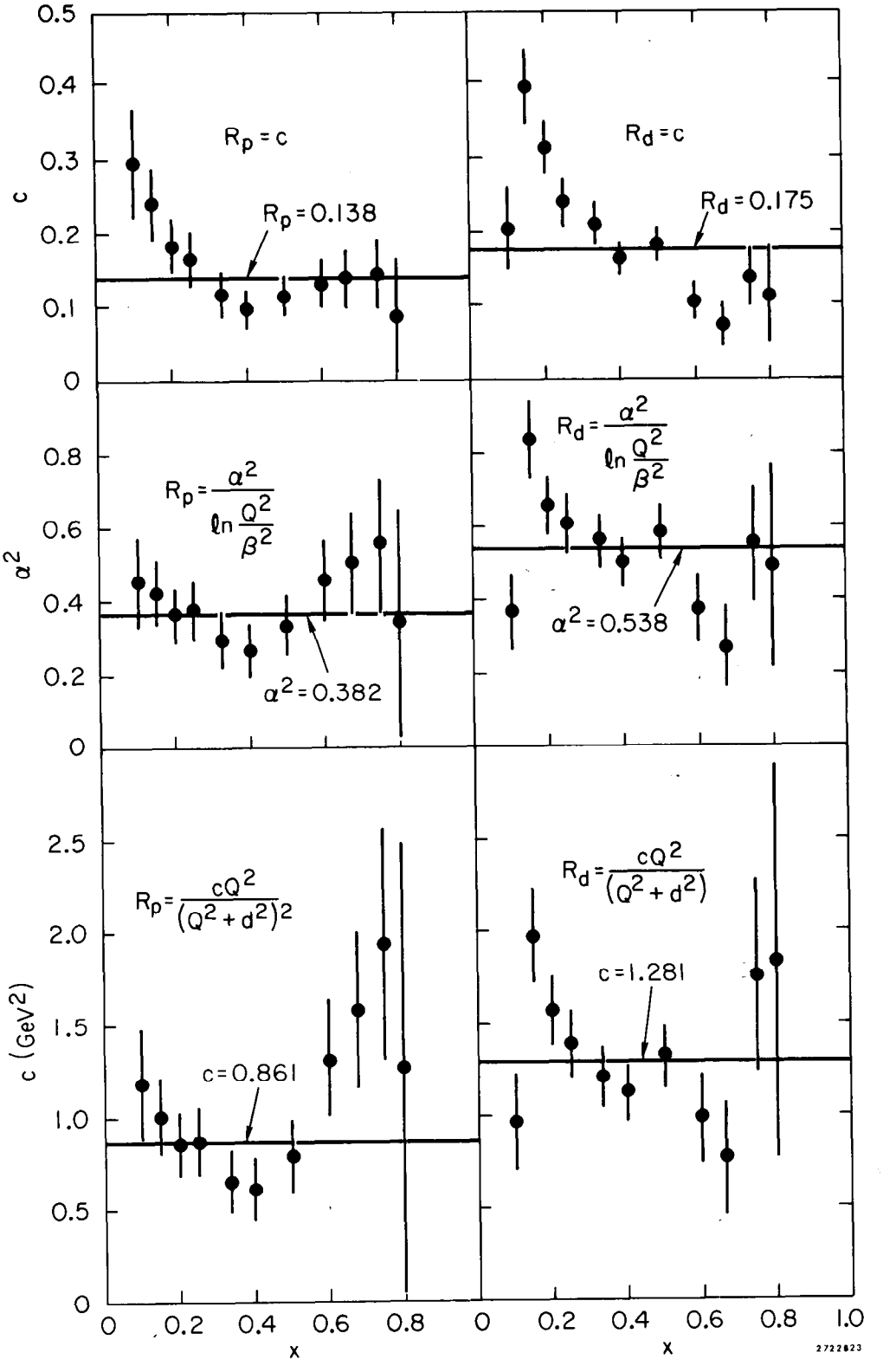

Fig. 31. Best-fit parameters of fixed - x fits to the R_p and R_d data. Errors shown are purely random.

either a constant, a $1/Q^2$, or a $1/\log Q^2$ dependence in the Bjorken limit. The present errors for R do not allow us to distinguish among these three functional forms.

The $x - Q^2$ array also permitted a study of the kinematic variation of νR_p and νR_d for fixed values of x. Light cone algebras with only spin-1/2 charged constituents predict[21, 22] that νR should scale, i.e., $\nu R(x,Q^2) = a(x)$. If there are charged spin-0 partons in the nucleon[23], then $\nu R(x,Q^2) = a(x) + \nu b(x)$, where $b(x)$ is the ratio of spin-0 to spin-1/2 contributions[69] to νW_2, in the limit of large Q^2. Other non-spin-1/2 contributions[67] to νW_2 would also result in a non-zero value of $b(x)$, as would also be expected in asymptotically-free field theories.[70]

In Figures (32,33) νR_p and νR_d are plotted versus Q^2 for fixed values of x between 0.1 and 0.8. The solid lines represent least square fits of the form $\nu R = a + b\nu = a + \frac{b}{2Mx}Q^2$. Best fit values of $b(x)$ and its random errors and systematic uncertainties are given in Table (XIV) for the eleven values of x studied. The five contributions to the systematic uncertainty in R_p and R_d also give uncertainties in the parameter b. The quadratic sum of the five such uncertainties in b is reported in Table (XIV) as Δb, the systematic uncertainty in b.

When these fits were restricted to $W \geq 2.0$ GeV, the best-fit values of b shifted by less than one standard deviation,

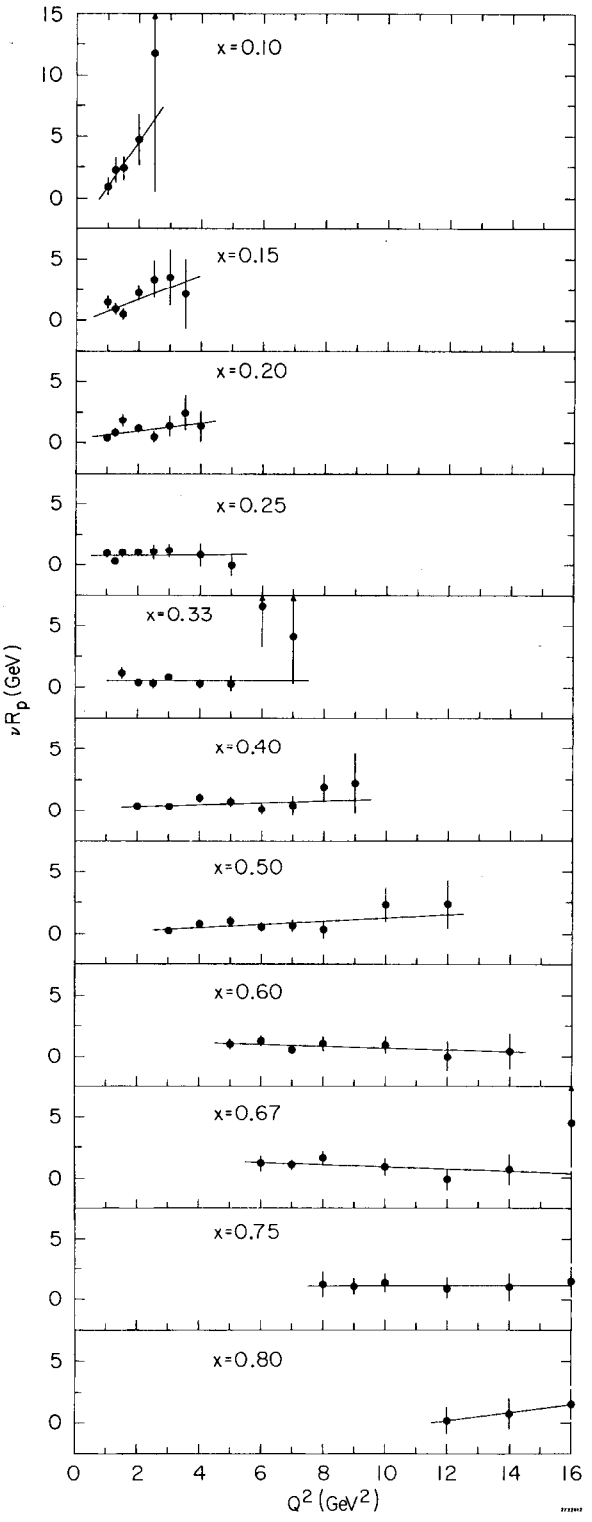

Fig. 32. The quantity νR_p plotted against Q^2 for the 11 fixed values of x studied.

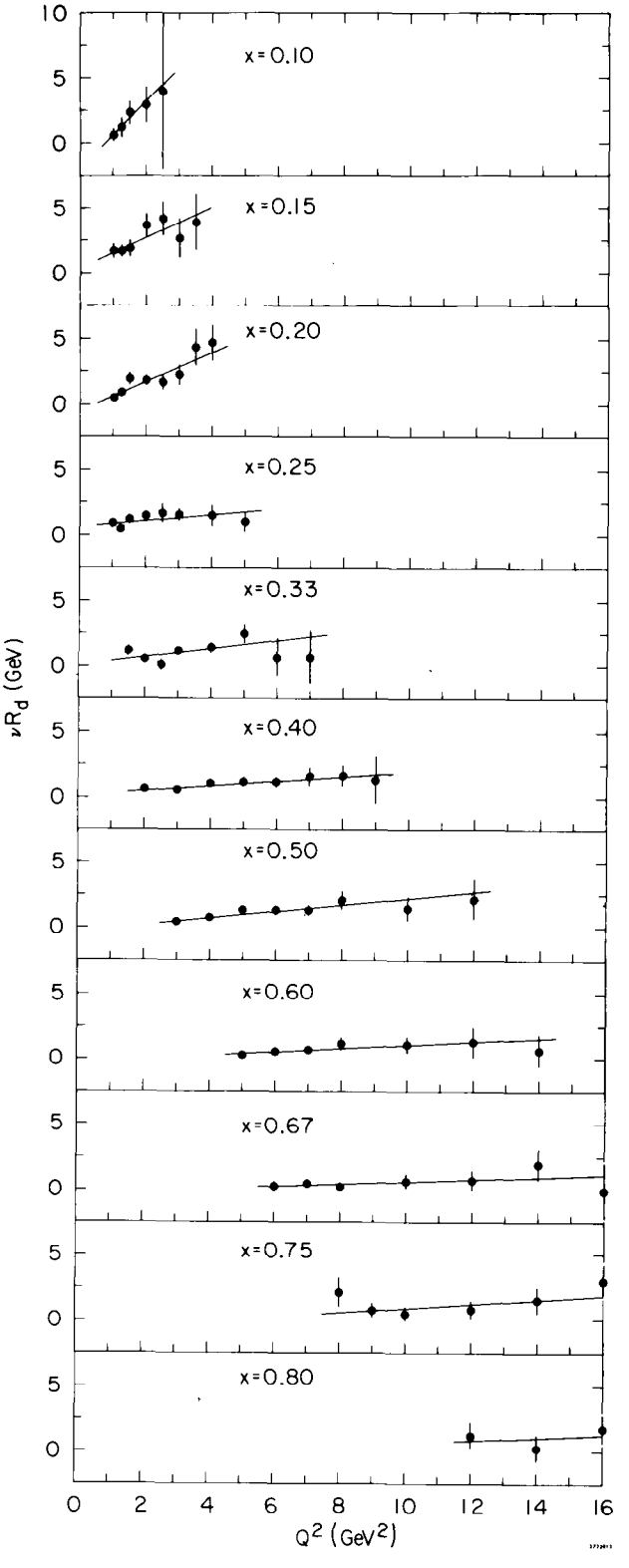

Fig. 33. The quantity νR_d plotted against Q^2 for the 11 fixed values of x studied.

Table XIV. Best-fit parameters b and their random errors and systematic uncertainties from least-square fits of the form $\nu R = a+b\nu$.

x	b_p	Δb_p	b_d	Δb_d
0.10	0.679 ± 0.330	0.130	0.478 ± 0.231	0.109
0.15	0.278 ± 0.166	0.111	0.331 ± 0.145	0.133
0.20	0.118 ± 0.090	0.058	0.415 ± 0.088	0.101
0.25	0.014 ± 0.084	0.033	0.108 ± 0.071	0.037
0.33	0.003 ± 0.098	0.030	0.195 ± 0.086	0.029
0.40	0.055 ± 0.066	0.032	0.129 ± 0.055	0.036
0.50	0.123 ± 0.075	0.034	0.234 ± 0.062	0.039
0.60	-0.087 ± 0.123	0.036	0.148 ± 0.096	0.038
0.67	-0.111 ± 0.148	0.049	0.114 ± 0.116	0.040
0.75	0.009 ± 0.221	0.031	0.233 ± 0.198	0.033
0.80	0.496 ± 0.642	0.049	0.169 ± 0.562	0.045

except at $x = 0.5$, where b_p shifted from 0.123 ± 0.075 to 0.023 ± 0.114, and b_d shifted from 0.234 ± 0.062 to 0.172 ± 0.089. When fits of the form $\nu R = a + b\nu$ were made to data for the $x - Q^2$ array restricted to experiments A and B, the results for b_p and b_d agreed with those of Table (XIV) within their random errors. For $0.25 \leq x \leq 0.80$, b_p is small and consistent with zero, within the random errors quoted. The average of b_p over this range of x is $\bar{b}_p = 0.035 \pm 0.036$ with an estimated systematic uncertainty of 0.033. Over this same range of x, b_d is frequently inconsistent with zero, within two standard deviations. Its average value over this range is $\bar{b}_d = 0.161 \pm 0.030$, with a systematic uncertainty of 0.037. The present results are consistent with the scaling of νR_p in this range of x, indicative of purely spin-1/2 constituents, in a parton model of the proton. The error in b, however, allows up to about a 10% spin-0 contribution to νW_2^p. The results are not consistent with scaling of νR_d. They are also consistent with about a 25% spin-0 contribution to νW_2^d. These spin-0 contributions would lead to non-vanishing values of R_p and R_d in the Bjorken limit.[23] Asymptotically-free field theories[18] are also consistent with these results, as they predict[70] a small increment above exact scaling behavior for νR. Large values of b are encountered for

$x \lesssim 0.2$, but a considerable portion of the data at these values of x is for $Q^2 \leq 2.0$ GeV^2, and the observed slope may represent only the low Q^2 turn-on[59] of νW_2. One could argue that the Fermi motion of the nucleons within the deuteron might lead to a non-zero value of b_d, while b_p remained equal to zero. But as discussed in Appendix (III), the approximate equality of the smearing ratios for W_1 and W_2 implies that smearing should have little effect upon R_d. Off-mass shell corrections to these smearing ratios are expected to reduce R_d at low Q^2 but these effects are estimated to increase b_d by about 0.01. It is presently unclear whether the behavior of νR_d at fixed x is indicative of a non-spin-1/2 contribution to inelastic e-d scattering or is due to some aspect of deuteron binding not now understood.

Recently, the Callan-Gross relation $R = Q^2/\nu^2$ (i.e., $F_2 = xF_1$) has been assumed in the analysis of neutrino experiments.[71] As indicated earlier, the parton model predicts $R = a(x)/\nu$ for general spin 1/2 constituents. The Callan-Gross relation is specifically for <u>unbound</u> constituents (i.e., $a(x) = Q^2/\nu = 2Mx$). We note that as $\nu \to \infty$, $R \to 0$ in either case and the relation $F_2 = xF_1$ is satisfied. Here we present the deviation

$$K = F_2/(xF_1) - 1 = \left(\nu^2/Q^2\right)\left[\frac{1+R}{1+\nu^2/Q^2}\right] - 1 \qquad \text{(VI.4)}$$

for the Q^2,ν range of this experiment. Figure (34) shows K averaged over Q^2 versus x for the proton and deuteron, and Figure (35) shows K averaged over x versus Q^2. Significant deviations from Callan-Gross are seen at low x and low Q^2. These deviations are expected and may come from binding effects of spin 1/2 constituents, low and high Q^2 non-scaling effects, or spin 0 constituents.

VI.D. Separation of the Structure Functions

At each kinematic point of the x - Q^2 array, the quantities $2MW_1$ and νW_2 were derived from σ_L and σ_T for both proton and deuteron according to equation (I.3). The separated values of $F_1(x,Q^2) = 2MW_1(x, Q^2)$ and $F_2(x,Q^2) = \nu W_2(x,Q^2)$ are reported in Table (XV), along with the random errors and relative systematic uncertainties in these quantities. Plots of $F_1(x,Q^2)$ and $F_2(x,Q^2)$ versus Q^2 for selected fixed values of x are presented in Figures (36) and (37) for both the proton and deuteron. The random errors in F_1 and F_2 were computed from the error matrix of the least-square fit to Σ, and therefore include a contribution from the random error in R at each point. As most of our cross section data were measured at values of ε between 0.6 and 0.9, this contribution is, in general, much larger for F_1 (corresponding to $\varepsilon = 0$) than for F_2 (corresponding to $\varepsilon = 1$). The relative uncertainties, which arise from the normalization uncertainties

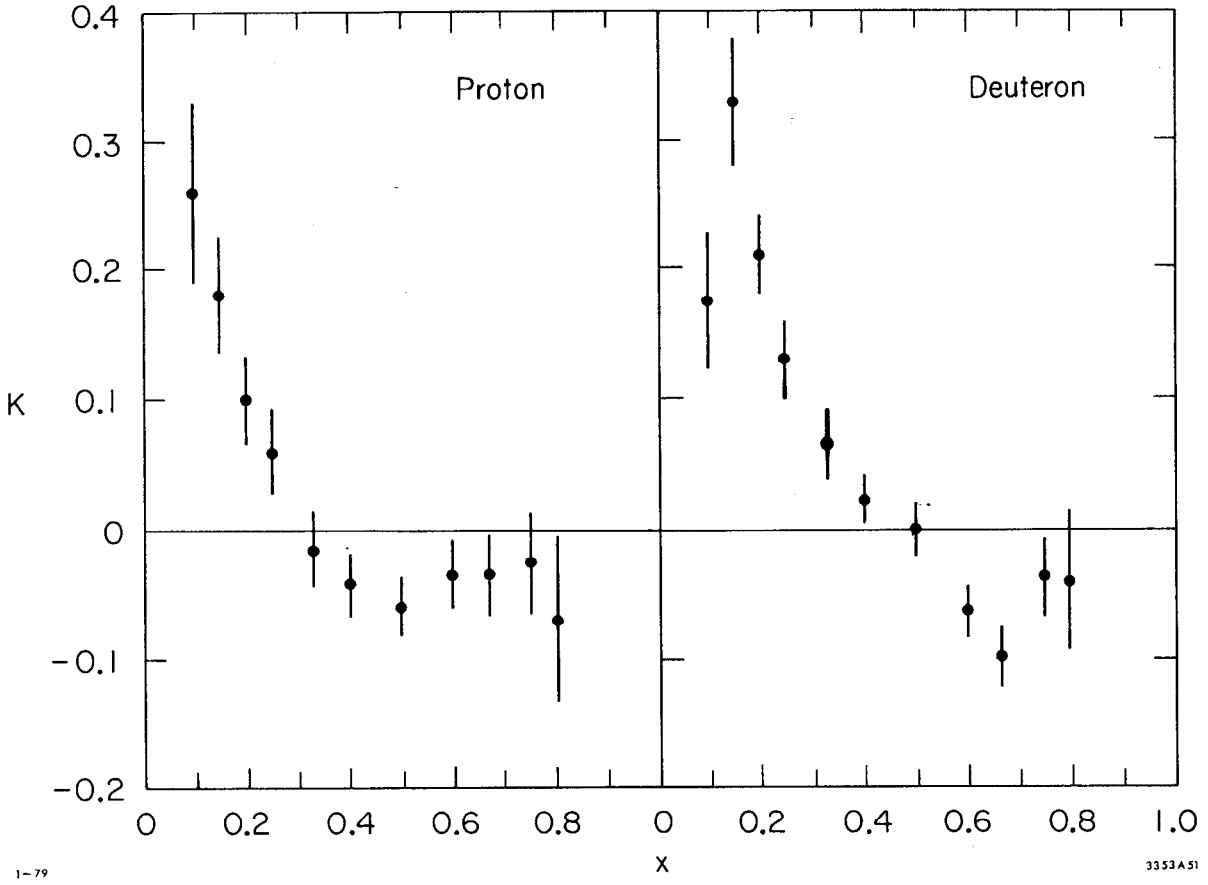

Fig. 34. Values of K, averaged over Q^2, plotted against x for the proton and deuteron. K is defined in equation VI.4.

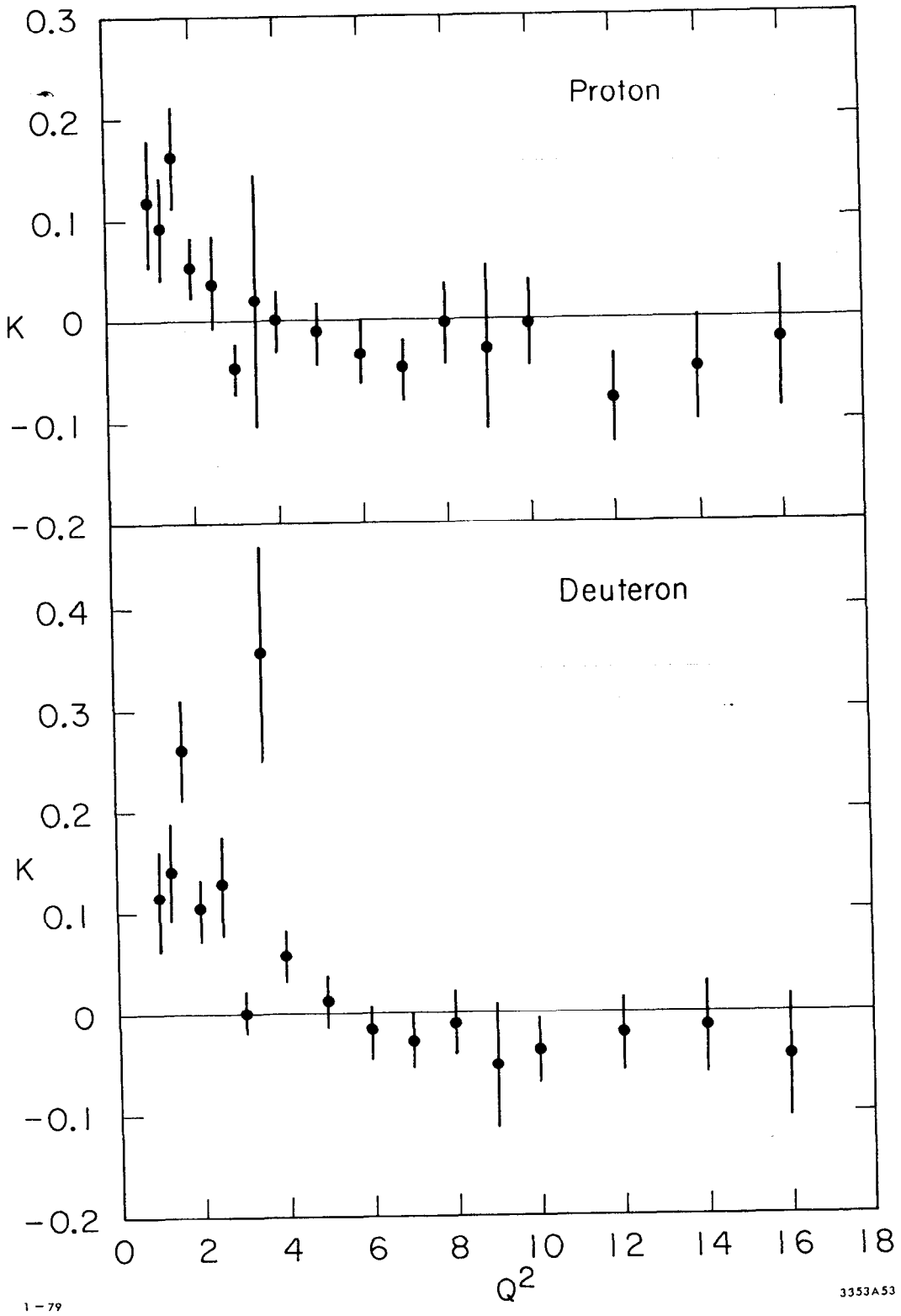

Fig. 35. Values of K, averaged over x, plotted against Q^2 for the proton and deuteron. K is defined in equation VI.4.

x	Q^2	$2MW_1^p$	Δ	νW_2^p	Δ	$2MW_1^d$	Δ	νW_2^d	Δ
0.10	1.00	2.7320±0.2435	0.2168	0.3100±0.0086	0.0088	5.3689±0.3524	0.4173	0.5808±0.0126	0.0206
0.10	1.25	2.5293±0.2333	0.2083	0.3291±0.0095	0.0092	5.3258±0.4165	0.4067	0.6120±0.0154	0.0205
0.10	1.50	2.6576±0.1983	0.2238	0.3381±0.0093	0.0095	5.0837±0.3422	0.4125	0.6402±0.0145	0.0215
0.10	2.00	2.5390±0.2401	0.2242	0.3598±0.0172	0.0099	5.1486±0.3443	0.4315	0.6441±0.0248	0.0225
0.10	2.50	2.3170±0.6479	0.2083	0.4295±0.0737	0.0193	5.2006±0.9577	0.5660	0.6649±0.1090	0.0451
0.15	1.00	1.6898±0.1661	0.1565	0.3308±0.0062	0.0098	2.9340±0.2830	0.2900	0.6032±0.0093	0.0217
0.15	1.25	1.9501±0.1395	0.1574	0.3315±0.0074	0.0101	3.1496±0.1921	0.2917	0.6118±0.0103	0.0230
0.15	1.50	2.1034±0.1369	0.1514	0.3283±0.0068	0.0096	3.2092±0.2393	0.2555	0.6216±0.0101	0.0219
0.15	2.00	1.8090±0.0937	0.1404	0.3448±0.0089	0.0102	2.9493±0.2033	0.2427	0.6459±0.0132	0.0236
0.15	2.50	1.7387±0.1546	0.1513	0.3617±0.0162	0.0143	3.0912±0.2153	0.2792	0.6613±0.0223	0.0330
0.15	3.00	1.8201±0.1803	0.1502	0.3544±0.0249	0.0146	3.5006±0.2277	0.2940	0.6407±0.0336	0.0345
0.15	3.50	1.9293±0.2252	0.1548	0.3321±0.0277	0.0147	3.4415±0.2787	0.2923	0.6649±0.0357	0.0369
0.20	1.00	1.5845±0.1287	0.1575	0.3183±0.0049	0.0089	2.7658±0.1911	0.3209	0.5720±0.0073	0.0197
0.20	1.25	1.4686±0.1173	0.1416	0.3288±0.0061	0.0097	2.5827±0.1845	0.2822	0.5880±0.0085	0.0213
0.20	1.50	1.2762±0.1070	0.1205	0.3399±0.0056	0.0098	2.2135±0.1557	0.2356	0.6000±0.0076	0.0212
0.20	2.00	1.4645±0.0710	0.1029	0.3333±0.0058	0.0093	2.4341±0.1128	0.1784	0.6076±0.0077	0.0205
0.20	2.50	1.6122±0.0776	0.1067	0.3270±0.0076	0.0098	2.5239±0.1466	0.1873	0.5986±0.0108	0.0221
0.20	3.00	1.5177±0.0948	0.1086	0.3394±0.0124	0.0124	2.5064±0.1276	0.1996	0.6113±0.0169	0.0277
0.20	3.50	1.4257±0.1150	0.1036	0.3457±0.0171	0.0132	2.2603±0.1571	0.1900	0.6367±0.0236	0.0303
0.20	4.00	1.4912±0.0967	0.1021	0.3247±0.0156	0.0130	2.2965±0.1345	0.1844	0.6385±0.0218	0.0312
0.25	1.00	1.0798±0.1275	0.1042	0.3184±0.0046	0.0087	1.8854±0.1832	0.3399	0.5509±0.0066	0.0186
0.25	1.25	1.3236±0.1200	0.1303	0.3112±0.0046	0.0088	2.1859±0.1662	0.2872	0.5500±0.0067	0.0191
0.25	1.50	1.1183±0.0962	0.1162	0.3188±0.0042	0.0088	1.8561±0.1320	0.2364	0.5575±0.0058	0.0189
0.25	2.00	1.1714±0.0662	0.0858	0.3253±0.0047	0.0087	1.8545±0.0985	0.1508	0.5623±0.0063	0.0184
0.25	2.50	1.1623±0.0920	0.0872	0.3195±0.0072	0.0095	1.8625±0.1642	0.1633	0.5634±0.0100	0.0206
0.25	3.00	1.1688±0.0612	0.0787	0.3211±0.0086	0.0100	1.9217±0.0848	0.1339	0.5559±0.0113	0.0207
0.25	4.00	1.1873±0.0792	0.0720	0.3082±0.0129	0.0100	1.9741±0.1030	0.1325	0.5493±0.0176	0.0223
0.25	5.00	1.2402±0.0653	0.0716	0.2959±0.0112	0.0103	2.0184±0.0838	0.1273	0.5295±0.0142	0.0236
0.33	1.50	0.7480±0.1035	0.1193	0.2016±0.0038	0.0079	1.2260±0.1298	0.2470	0.4827±0.0053	0.0163
0.33	2.00	0.8939±0.0505	0.0877	0.2794±0.0033	0.0071	1.4293±0.0659	0.1277	0.4676±0.0046	0.0146
0.33	2.50	0.8863±0.0734	0.0749	0.2756±0.0043	0.0076	1.5366±0.1389	0.1451	0.4559±0.0062	0.0157
0.33	3.00	0.8064±0.0316	0.0467	0.2799±0.0039	0.0070	1.2626±0.0401	0.0777	0.4622±0.0051	0.0145
0.33	4.00	0.8449±0.0331	0.0449	0.2674±0.0057	0.0072	1.2266±0.0442	0.0733	0.4534±0.0080	0.0146
0.33	5.00	0.8084±0.0452	0.0435	0.2600±0.0080	0.0078	1.1362±0.0569	0.0750	0.4590±0.0106	0.0164
0.33	6.00	0.5898±0.0765	0.0312	0.3114±0.0243	0.0069	1.2554±0.0927	0.0603	0.4201±0.0301	0.0092
0.33	7.00	0.6487±0.0857	0.0323	0.2795±0.0336	0.0063	1.2306±0.1015	0.0588	0.4124±0.0401	0.0094
0.40	2.00	0.6927±0.0464	0.0578	0.2464±0.0028	0.0062	1.0314±0.0573	0.1054	0.3985±0.0038	0.0118
0.40	3.00	0.6342±0.0250	0.0356	0.2303±0.0032	0.0055	0.9751±0.0299	0.0594	0.3732±0.0042	0.0109
0.40	4.00	0.5570±0.0252	0.0309	0.2331±0.0041	0.0057	0.8831±0.0302	0.0516	0.3700±0.0054	0.0117
0.40	5.00	0.5683±0.0229	0.0272	0.2259±0.0049	0.0054	0.8589±0.0277	0.0433	0.3610±0.0062	0.0097
0.40	6.00	0.5731±0.0228	0.0259	0.2118±0.0044	0.0052	0.8422±0.0257	0.0421	0.3521±0.0054	0.0099
0.40	7.00	0.5430±0.0280	0.0238	0.2001±0.0082	0.0056	0.8108±0.0314	0.0358	0.3501±0.0098	0.0079
0.40	8.00	0.4982±0.0261	0.0218	0.2170±0.0088	0.0058	0.7907±0.0290	0.0343	0.3399±0.0105	0.0079
0.40	9.00	0.4746±0.0401	0.0205	0.2104±0.0202	0.0048	0.7868±0.0476	0.0335	0.3289±0.0246	0.0074
0.50	3.00	0.4129±0.0194	0.0248	0.1714±0.0021	0.0040	0.6160±0.0228	0.0417	0.2679±0.0028	0.0075
0.50	4.00	0.3439±0.0167	0.0182	0.1677±0.0028	0.0037	0.5286±0.0188	0.0302	0.2558±0.0038	0.0072
0.50	5.00	0.3166±0.0164	0.0153	0.1593±0.0029	0.0033	0.4644±0.0183	0.0236	0.2454±0.0036	0.0056
0.50	6.00	0.3181±0.0134	0.0136	0.1505±0.0027	0.0033	0.4516±0.0156	0.0217	0.2380±0.0034	0.0060
0.50	7.00	0.3014±0.0136	0.0135	0.1453±0.0029	0.0031	0.4365±0.0150	0.0210	0.2279±0.0033	0.0055
0.50	8.00	0.2974±0.0159	0.0115	0.1392±0.0047	0.0026	0.4080±0.0176	0.0163	0.2285±0.0056	0.0042
0.50	10.00	0.2555±0.0160	0.0112	0.1429±0.0067	0.0030	0.4063±0.0174	0.0163	0.2124±0.0075	0.0045
0.50	12.00	0.2501±0.0173	0.0095	0.1379±0.0083	0.0033	0.3823±0.0205	0.0143	0.2084±0.0104	0.0048
0.60	5.00	0.1736±0.0114	0.0082	0.1023±0.0018	0.0020	0.2902±0.0130	0.0126	0.1470±0.0023	0.0028
0.60	6.00	0.1601±0.0085	0.0072	0.0983±0.0018	0.0020	0.2542±0.0094	0.0111	0.1395±0.0021	0.0030
0.60	7.00	0.1624±0.0070	0.0068	0.0900±0.0015	0.0020	0.2338±0.0078	0.0106	0.1319±0.0017	0.0033
0.60	8.00	0.1484±0.0081	0.0055	0.0884±0.0022	0.0017	0.2142±0.0093	0.0078	0.1290±0.0026	0.0024
0.60	10.00	0.1370±0.0068	0.0047	0.0809±0.0021	0.0016	0.1994±0.0083	0.0067	0.1188±0.0027	0.0022
0.60	12.00	0.1335±0.0081	0.0045	0.0726±0.0046	0.0016	0.1882±0.0097	0.0064	0.1144±0.0056	0.0024
0.60	14.00	0.1252±0.0072	0.0042	0.0712±0.0041	0.0016	0.1807±0.0088	0.0057	0.1047±0.0050	0.0022
0.67	6.00	0.0997±0.0085	0.0042	0.0653±0.0014	0.0012	0.1651±0.0099	0.0065	0.0929±0.0018	0.0017
0.67	7.00	0.0937±0.0051	0.0039	0.0604±0.0011	0.0012	0.1469±0.0060	0.0059	0.0868±0.0013	0.0018
0.67	8.00	0.0861±0.0048	0.0031	0.0597±0.0013	0.0013	0.1392±0.0054	0.0046	0.0804±0.0015	0.0015
0.67	10.00	0.0813±0.0044	0.0028	0.0519±0.0015	0.0009	0.1182±0.0052	0.0039	0.0737±0.0017	0.0013
0.67	12.00	0.0784±0.0043	0.0029	0.0455±0.0019	0.0008	0.1069±0.0050	0.0037	0.0677±0.0021	0.0012
0.67	14.00	0.0699±0.0040	0.0022	0.0444±0.0022	0.0009	0.0960±0.0048	0.0030	0.0677±0.0027	0.0014
0.67	16.00	0.0573±0.0074	0.0018	0.0470±0.0039	0.0010	0.0980±0.0090	0.0029	0.0592±0.0047	0.0012
0.75	8.00	0.0411±0.0051	0.0016	0.0300±0.0010	0.0006	0.0537±0.0064	0.0022	0.0445±0.0012	0.0008
0.75	9.00	0.0389±0.0028	0.0013	0.0279±0.0006	0.0005	0.0580±0.0034	0.0019	0.0400±0.0008	0.0007
0.75	10.00	0.0359±0.0024	0.0012	0.0267±0.0008	0.0005	0.0550±0.0028	0.0018	0.0369±0.0009	0.0006
0.75	12.00	0.0332±0.0020	0.0012	0.0237±0.0009	0.0004	0.0480±0.0023	0.0016	0.0339±0.0009	0.0006
0.75	14.00	0.0294±0.0018	0.0009	0.0213±0.0010	0.0004	0.0415±0.0022	0.0012	0.0314±0.0012	0.0006
0.75	16.00	0.0264±0.0016	0.0008	0.0199±0.0009	0.0004	0.0361±0.0019	0.0011	0.0305±0.0011	0.0006
0.80	12.00	0.0194±0.0018	0.0006	0.0133±0.0006	0.0002	0.0263±0.0020	0.0008	0.0204±0.0007	0.0003
0.80	14.00	0.0169±0.0014	0.0005	0.0125±0.0006	0.0002	0.0252±0.0016	0.0007	0.0179±0.0008	0.0003
0.80	16.00	0.0145±0.0010	0.0004	0.0116±0.0005	0.0002	0.0212±0.0012	0.0006	0.0173±0.0006	0.0003

2722C25

Table XV. Separated values of $2MW_1$ and νW_2 and their random errors and relative systematic uncertainties.

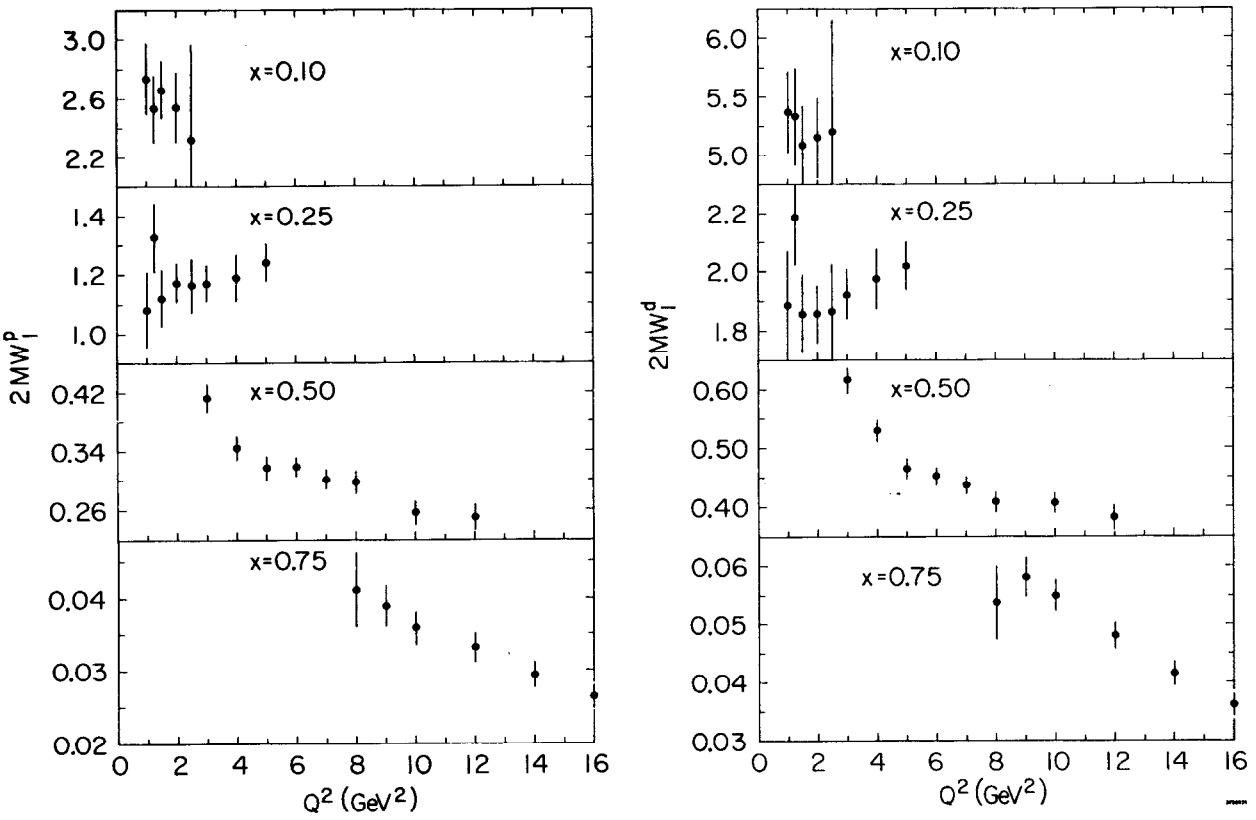

Fig. 36. Separated values of $2MW_1 = F_1(x, Q^2)$ for the proton and deuteron plotted against Q^2 for fixed values of x. The errors shown are purely random.

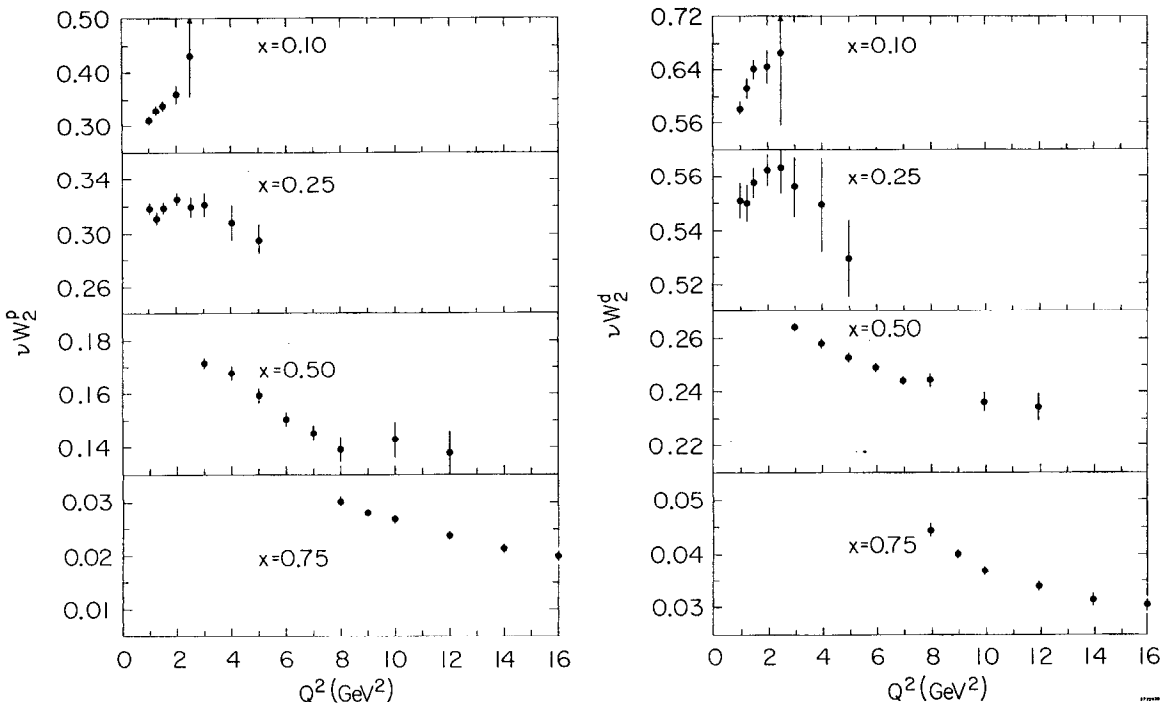

Fig. 37. Separated values of $\nu W_2 = F_2(x, Q^2)$ for the proton and deuteron plotted against Q^2 for fixed values of x. The errors shown are purely random.

and from the cross section uncertainties listed in Table (VII), are those which can affect the Q^2-dependence of F_1 and F_2. They were estimated in a manner similar to that used to estimate the uncertainties in R, and were added in quadrature to produce the numbers listed under Δ in Table (XV). The relative uncertainty arising from the uncertainty in the radiative corrections ranged from 2% to 10% in F_1 and from 1.5% to 2% in F_2. Overall normalization uncertainties in F_1 and F_2, arising from the cross section uncertainties of Table (VII), are estimated to be 3.4% for the proton structure functions and 3.6% for the deuteron.